

Article

Strategic Synthesis to Disperse Zeolite NaY in Lead Tree Wood

Panot Krukkratoke ¹, Chalermpan Keawkumay ^{1,2} , Pimwipa Tayraukham ¹, Kewalee Prompiputtanapon ³, Pongtanawat Khemthong ⁴ , Sanchai Prayoonpokarach ¹  and Jatuporn Wittayakun ^{1,*}

¹ School of Chemistry, Institute of Science, Suranaree University of Technology, Nakhon Ratchasima 30000, Thailand; notzsone@gmail.com (P.K.); chalermpan@sut.ac.th (C.K.); pimwipatr@gmail.com (P.T.); sanchaip@sut.ac.th (S.P.)

² Institute of Research and Development, Suranaree University of Technology, Nakhon Ratchasima 30000, Thailand

³ The Center for Scientific and Technological Equipment, Suranaree University of Technology, Nakhon Ratchasima 30000, Thailand; kewalee@sut.ac.th

⁴ National Nanotechnology Center (NANOTEC), National Science and Technology Development Agency (NSTDA), Pathumthani 12120, Thailand; pongtanawat@nanotec.or.th

* Correspondence: jatuporn@sut.ac.th; Tel.: +66-44-224-256

Abstract: The goal of this work is to synthesize zeolite NaY inside Lead tree wood. The wood is mixed with zeolite seed gel before mixing with feed gel and subsequent hydrothermal treatment. In the first trial, the dried and untreated Lead tree wood is mixed with the gel of zeolite NaY before the hydrothermal process. Only zeolite NaP is produced. Then, sonication is applied to the wood and zeolite gel mixture before the hydrothermal process. The product is mixed with the phase of NaP and NaY. In the next attempt, the wood is treated with acid reflux before mixing with the zeolite seed gel. NaY is successfully produced inside the wood. When sonication is also applied, the amount of NaY is increased. The presence of zeolites in the wood are confirmed by X-ray diffraction, scanning electron microscopy, nitrogen adsorption, and thermogravimetric analysis. Moreover, the composites are tested for the adsorption of nickel (II) ions from aqueous solutions. The novel Lead tree wood-zeolite NaY composite has the potential as an adsorbent which could be separated easily from the liquid media.

Keywords: wood-zeolite composite; lead tree wood; zeolite NaY; zeolite NaP; sonication; acid treatment



Citation: Krukkratoke, P.; Keawkumay, C.; Tayraukham, P.; Prompiputtanapon, K.; Khemthong, P.; Prayoonpokarach, S.; Wittayakun, J. Strategic Synthesis to Disperse Zeolite NaY in Lead Tree Wood. *Crystals* **2022**, *12*, 504. <https://doi.org/10.3390/cryst12040504>

Academic Editor: Sergio Brutti

Received: 28 February 2022

Accepted: 1 April 2022

Published: 5 April 2022

Publisher's Note: MDPI stays neutral with regard to jurisdictional claims in published maps and institutional affiliations.



Copyright: © 2022 by the authors. Licensee MDPI, Basel, Switzerland. This article is an open access article distributed under the terms and conditions of the Creative Commons Attribution (CC BY) license (<https://creativecommons.org/licenses/by/4.0/>).

1. Introduction

Adsorption is a simple process to remove pollutants from aqueous [1–6] or gaseous [7,8] systems. The desired adsorbents are generally low-cost or generated from renewable sources. Common adsorbents are zeolites [1,9,10] and biomass-derived materials [11]. Moreover, the composites between biomass and zeolites have been explored.

Zeolites are crystalline aluminosilicate materials with the formula $\text{Na}_x[(\text{AlO}_2)_x(\text{SiO}_2)_y] \cdot n\text{H}_2\text{O}$. Zeolites are widely used because they have large surface areas, pore volumes, and ion exchange sites for adsorption [12,13]. One of the most common types of zeolites is NaY. However, zeolite in the powder form is difficult to separate from the liquid media after the adsorption process [14]. The dispersion of zeolite in wood could make the separation more convenient.

The wood of interest in this study is the Lead tree (*Leucaena leucocephala* de Wit). It is a fast-growing plant abundant in many parts of the world, including Thailand [15]. The wood has a porous structure that could serve as a support to disperse zeolites.

The objective of this work is to synthesize zeolite NaY in Lead tree wood. The strategies to achieve this goal include sonication of the wood-zeolite gel mixture and treating the wood with acid before the synthesis. Here we report the outcome of each strategy to produce the novel Lead tree wood-zeolite NaY composite. This approach demonstrates the sustainable utilization of Lead tree wood for further application.

2. Materials and Methods

2.1. Chemicals and Materials

Lead tree wood (LW) was collected at the Suranaree University of Technology campus. The bark was removed and the wood was chopped to the length of 30 cm before drying at 90 °C for 96 h. The dried LW was cut into pellets with a height of 0.5 cm and diameter of 1.0 cm. The dried LW pellets were further dried at 90 °C for 24 h.

In the case of acid treatment, approximately 5.00 g of LW pellets were mixed with 67 mL of 3 M HCl (prepared from 37% HCl, ANAPURE®, Auckland, New Zealand) in a round-bottom flask, refluxed at 90 °C for 6 h and cooled down to ambient temperature. The pellets were separated by filtration, washed with DI water until the filtrate was neutral and dried at 90 °C for 24 h.

2.2. Synthesis of Lead Tree Wood-Zeolite NaY Composites

In the synthesis of Lead tree wood-zeolite composites, seed and feed gels of zeolite NaY were prepared by a procedure from the literature [16] from fumed silica (99.8% SiO₂, Sigma-Aldrich, St. Louis, MO, USA), sodium aluminate (50–56% Al₂O₃, 40–45% Na₂O, Sigma-Aldrich Chemie GmbH, Steinheim, Germany), sodium hydroxide (97% wt NaOH, Carlo Erba, Val de reuil, France). The molar composition of the overall gel was 4.62Na₂O:1Al₂O₃:10SiO₂:180H₂O.

One gram of LW was added to a solution containing 1.00 g NaOH in 10.00 mL of DI water in a centrifuge tube, capped, and aged at ambient temperature for 24 h. The mixture was transferred into a Teflon bottle, added with 0.42 g of anhydrous NaAlO₂, stirred until homogeneous, and finally added with 4.80 g of Na₂SiO₃. The final mixture, seed gel with a molar composition of 10.57Na₂O:1Al₂O₃:10.56SiO₂:332H₂O was stirred for 10 min, capped, and aged at room temperature for 24 h.

The feedstock gel with a molar position of 4.67Na₂O:1Al₂O₃:10SiO₂:158H₂O was prepared by dissolving 2.7820 g of anhydrous NaAlO₂ into a solution containing 0.035 g of NaOH in 22.3 mL of DI water. After that, the mixture was added to 30.19 g of Na₂SiO₃ solution and stirred for 10 min.

Finally, the feedstock gel was added to the LW-containing seed gel, stirred for 10 min, and aged in a closed container at ambient temperature for 24 h. The overall gel was further crystallized under the hydrothermal condition at 90 °C for 24 h. After cooling down, the LW pellets were removed from the mixture, added with DI water and sonicated for 10 min in a sonication bath. This step was performed repeatedly until the washing water was neutral. The composites from the untreated and refluxed wood were named NR and R, respectively.

In the separate synthesis, the freshly-prepared overall gel was sonicated immediately according to the procedure adapted from Sosa et al. [17] using an ultrasonic probe (Sonics Vibra-Cell: VCX 130, Sonics & Materials, Inc., Newtown, CT, USA) with a probe size of 6 mm. With the frequency of 20 kHz and a power of 130 W, an on-off pulse was set at 5 s in 30 min. After that, the gel was aged and crystallized under the conditions above. The obtained composites from untreated and refluxed wood with sonication are named NRS and RS, respectively.

2.3. Characterization

Phases of the composites were analyzed by X-ray diffraction (XRD) on a Bruker D8 ADVANCE (Bruker AXS GmbH, Karlsruhe, Germany) with Cu Kα radiation operated at a voltage and current of 40 kV and 30 mA. The scan speed was 0.2 s/step and the increment was 0.02 s/step.

Morphology and elemental analysis of the composites were analyzed by scanning electron microscopy with energy dispersive X-ray spectroscopy (SEM-EDS, Carl Zeiss, Auriga® series, Carl Zeiss NTS GmbH, Oberkochen, Germany) with accelerating voltage of 30 kV. The samples were spread on silver paint and coated with gold by sputtering.

Nitrogen adsorption isotherms of the composites were acquired from a BELSORP-mini II (BEL Japan, Inc., Osaka, Japan) at liquid nitrogen temperature. The samples (approx-

imately 120 mg) were degassed at 70 °C for 24 h before the measurement. The specific surface areas (S_{BET}) were calculated using the Brunauer-Emmett-Teller (BET) equation.

The thermal decomposition of the composites (approximately 15 mg) was studied by thermogravimetric analysis (TGA) on a Mettler Toledo model TGA/DSC1 (Mettler-Toledo AG, Analytical, Schwerzenbach, Switzerland) with air-zero. A gas flow rate was 50 mL/min and a heating rate was 10 °C/min up to 800 °C. After the wood was burnt out, the remaining residues were assumed to consist mainly of zeolite.

2.4. Adsorption Experiment

Batch experiments were carried out to investigate the ability of the zeolite-wood composites on the adsorption of Ni(II) ions. One pellet of each adsorbent was added to 20 mL of Ni(II) solution (100 mg/L) in a 125 mL Erlenmeyer flask, and stirred at 400 rpm for 3 h to ensure equilibrium. After the experiment, the pellet was easily picked out from the media. The remaining concentration of Ni(II) was determined using flame atomic absorption spectrophotometry (PerkinElmer, PinAAcle 900F, PerkinElmer, Inc., Waltham, MA, USA). The amount of Ni(II) adsorbed at equilibrium (q_e) was calculated by the equation below.

$$q_e = \frac{(C_0 - C_e) \times V}{w}$$

C_0 and C_e are the initial and equilibrium concentration of Ni(II), respectively. V is the volume of the solution (L) and w is the amount of adsorbent (g).

3. Results and Discussion

3.1. Characterization of Untreated (NR) and Refluxed (R) Lead Tree Wood

Figure 1a–c shows photographs, XRD pattern and SEM image of untreated Lead tree wood (LW) pellets after drying. The XRD pattern displays peaks at 14° and 22°, which are characteristic of 110 and 200 planes of cellulose, respectively [18]. The broad peaks indicate an amorphous nature. The SEM image of the untreated LW (Figure 1c) shows a vascular system on the cortex with large pores (around 10–12 mm) and a smooth surface. The pore size of LW is similar to the work by Pimsuta [19].

Figure 1d–f shows photographs, XRD pattern and SEM image of refluxed LW. The refluxed pellets are smaller in both height and diameter and have a darker color than the untreated samples. The XRD pattern has the same peak positions but with the decrease of the peak of 200 plane. The changes are from hydrolysis by acid, which causes depolymerization of the lignocellulose [20]. However, significant changes in morphology of LW and refluxed LW are not observed from the SEM images.

3.2. Characterization of Untreated Lead Tree Wood-Zeolite Composites

Figure 2 shows the pictures of all the wood-zeolite composites. The NR sample has a rougher surface with a diameter of about 0.7 cm, which is smaller than the untreated wood. On the other hand, the NRS sample looks similar to the untreated wood with little swelling. These samples show more shrinkage in the middle of the pellet. This could lead to smaller vascular pore sizes.

The composites R and RS show more shrinkage of about 0.5 cm. The pith of these samples shows more deflation than the NR and NRS. The side view of these samples shows the pellet with an even width. Refluxing the wood seems to improve the diffusion of zeolite precursors throughout the pellet.

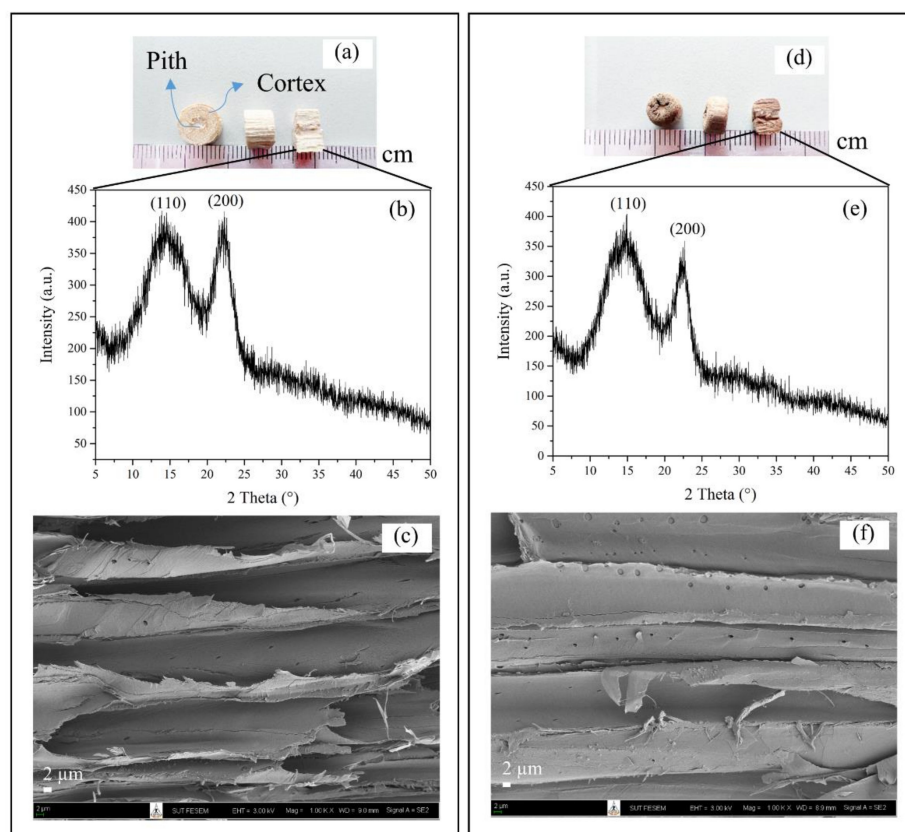


Figure 1. (a) Photographs of untreated Lead tree wood (LW) pellets, from left to right showing the pith and cortex from the top view, the side view and cross section; (b,c) XRD pattern and SEM image of the LW cross section; (d) photographs of refluxed LW pellets, from left to right showing the top view, the side view and cross section; (e,f) XRD pattern and SEM image of the refluxed LW cross section.



Figure 2. Top-view (a) and side-view (b) photographs of Lead tree wood-zeolite composites of (from left to right) untreated wood (NR), untreated wood with sonication (NRS), refluxed wood (R) and refluxed wood with sonication (RS).

Figure 3a shows the XRD pattern of the NR composite. The uneven background could be from the uneven surface of the sample, which was prepared by slitting through the pellet. The characteristic peaks of cellulose are observed at around 14 and 22 degrees. Moreover, the peaks which are characteristics of zeolite NaP (12°, 18°, 22°, 28°, and 33°) are observed [21]. This result demonstrates that zeolite NaP could be produced inside LW from the gel of NaY under the same condition. Previously, NaP was produced from the gel of NaY but with a longer crystallization time or higher hydrothermal temperature [22–24]. To our best knowledge, this is the first report that NaP has been dispersed inside the wood.

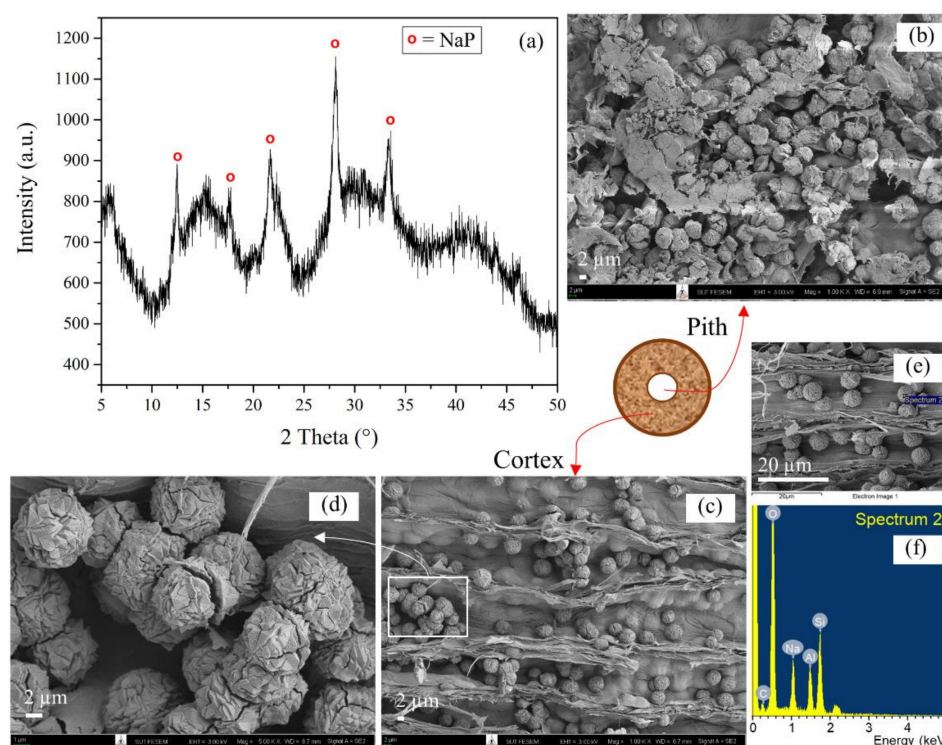


Figure 3. (a) XRD patterns, SEM images of Lead tree wood-zeolite composites of untreated wood (NR) (b) at pith, (c,d) at cortex, and (e,f) EDS points analysis spectrum.

The SEM images of NR at the pith and cortex are shown in Figure 3b–d, respectively. At low magnification, both parts show spherical particles with a size of around 3–5 µm dispersed in the pores of LW. The image from high magnification shows that each particle has polycrystals with cracks. Such a morphology is similar to that of zeolite NaP in the literature [23] and is in good agreement with the XRD result. The EDS point analysis spectrum is shown in Figure 3e,f. The Si/Al ratio of this sample is 2.25.

In the absence of wood, the formation of NaP from the gel composition of zeolite NaY was explained by Shirazian et al. [25]. The crystallization rate of zeolite NaP is faster than that of zeolite NaY. With the presence of Lead tree wood, there are two possible explanations. When the wood is mixed with an alkaline solution, some water could be absorbed by the wood, resulting in the higher alkalinity of the media. Such a condition may lead to faster crystallization. Another possibility is that the roughness in the wood pores serves as a nucleation site for crystallization.

Figure 4a shows the XRD pattern of the NRS composite. The characteristic peaks of zeolite NaP are observed along with the peak at 6°, which is the strongest peak of NaY [26]. With the use of sonication, the zeolite precursors may diffuse better into the wood. As a result, some gel compositions are suitable for the formation of NaY, but the majority is still NaP. The SEM image with low magnification (Figure 4b) and higher magnification at pith and cortex (Figure 4c–e), respectively, shows spherical morphology. The zoom-in of the particles shows cracked polycrystals with a diameter of around 3–5 µm. These particles look similar to NaP in the NR composite. Moreover, polyhedral particles

with a size of 0.5–4 μm are observed. These particles are similar to those of zeolite NaY in the literature [27]. This mixed morphology of NaP and NaY agrees with the XRD result. The EDS point analysis spectra at polyhedral and polycrystal particles (Figure 4f,g and Figure 4h,i, respectively) give Si/Al ratio of 2.39 and 2.74, respectively.

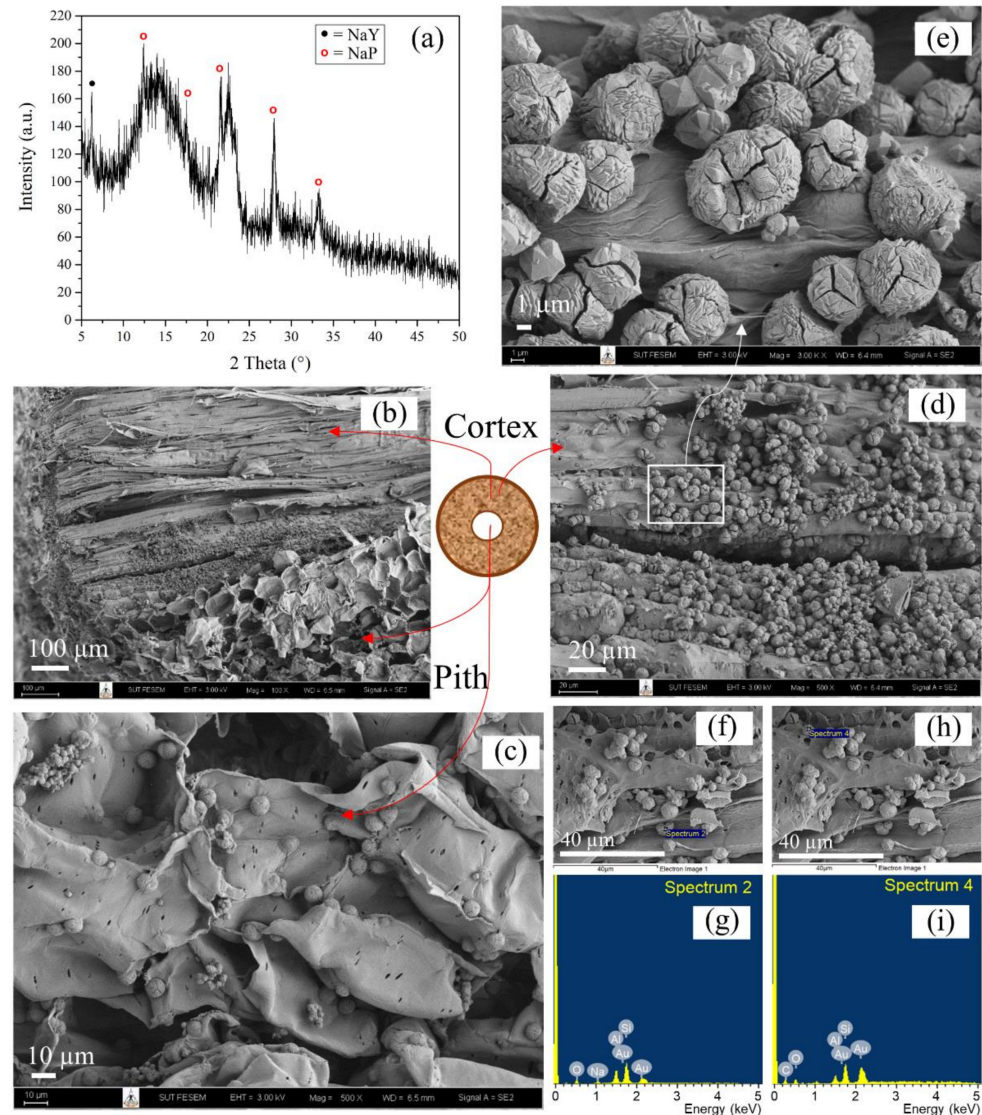


Figure 4. (a) XRD patterns, (b) SEM images Lead tree wood-zeolite composites of untreated wood with sonication (NRS) (c) at pith, (d,e) at cortex, and EDS points analysis spectrum of (f,g) polyhedral and (h,i) three pointed cracked spherical morphology, respectively.

3.3. Characterization of Refluxed Lead Tree Wood-Zeolite Composites

Figure 5a shows the XRD pattern of the R composite. The characteristic peaks of zeolite NaY at 6° , 16° , 24° , 27° , and 31° are clearly observed [26]. This result confirmed that zeolite NaY inside LW can be produced from the gel of NaY. The reflux with acid could clear the wood pores, which allows the zeolite precursors to diffuse more easily into the middle of the wood. The gel composition inside the wood is similar to the regular gel composition to form NaY. This is the first report that zeolite NaY is produced inside a wood material.

SEM images of the R composite are shown in Figure 5b–d at the pith and cortex, respectively. Both single crystals and polycrystals are observed. The EDS point analysis spectrum of this sample gives a Si/Al ratio of 2.16.

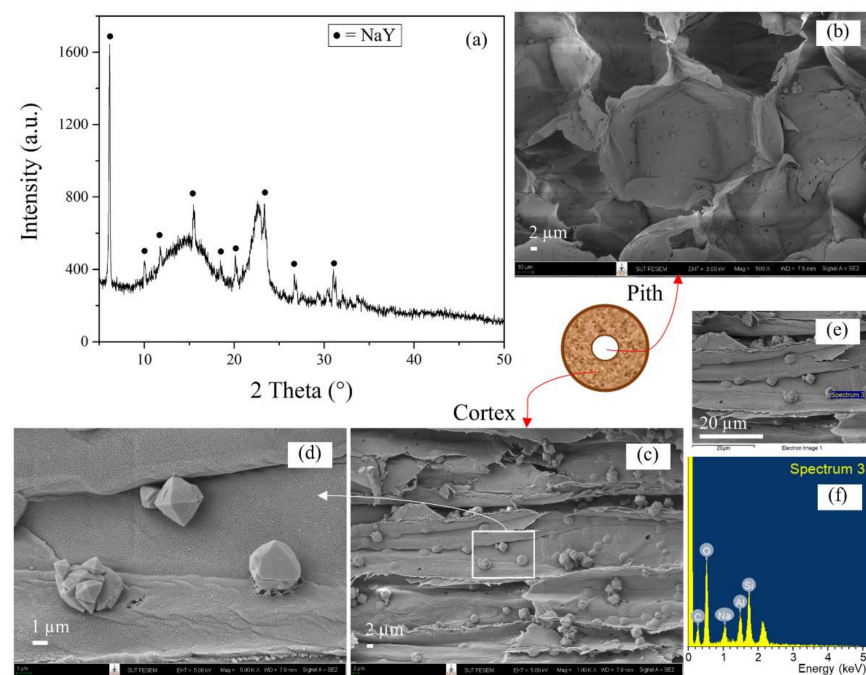


Figure 5. (a) XRD patterns, SEM images of Lead tree wood-zeolite composites of refluxed wood (R) (b) at pith, (c,d) at cortex, and (e,f) EDS points analysis spectrum.

Figure 6a shows the XRD pattern of the RS sample. The characteristic peaks of zeolite NaY are observed. The intensity of the main peak at 6° from this sample is much stronger than that from the R composite. The results indicate that higher amounts of NaY are produced in this sample, which could be a combinative effect of wood refluxing and sonication. Refluxing the wood might clear and expand the wood pores, which are easier for diffusion. The sonication then increases the diffusion throughout the wood.

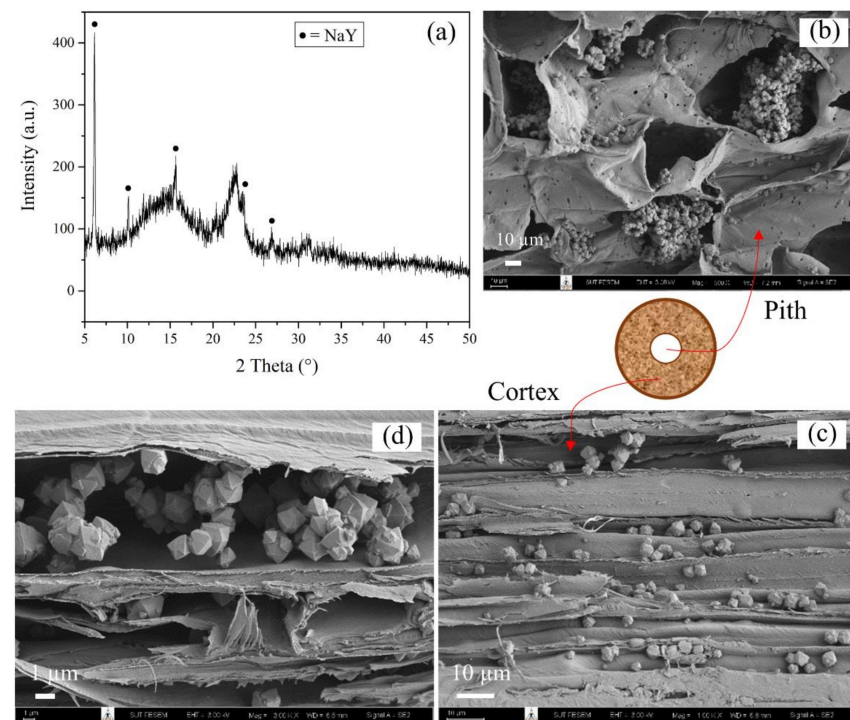


Figure 6. (a) XRD patterns, SEM images of refluxed wood-zeolite composites with sonication (RS) (b) at pith, and (c,d) at cortex.

The SEM images of RS at the pith and cortex are shown in Figure 6b and Figure 6c,d, respectively. Polycrystals with polyhedral morphology are observed. The EDS point analysis spectrum in Figure 7 gives a Si/Al ratio of 2.16.

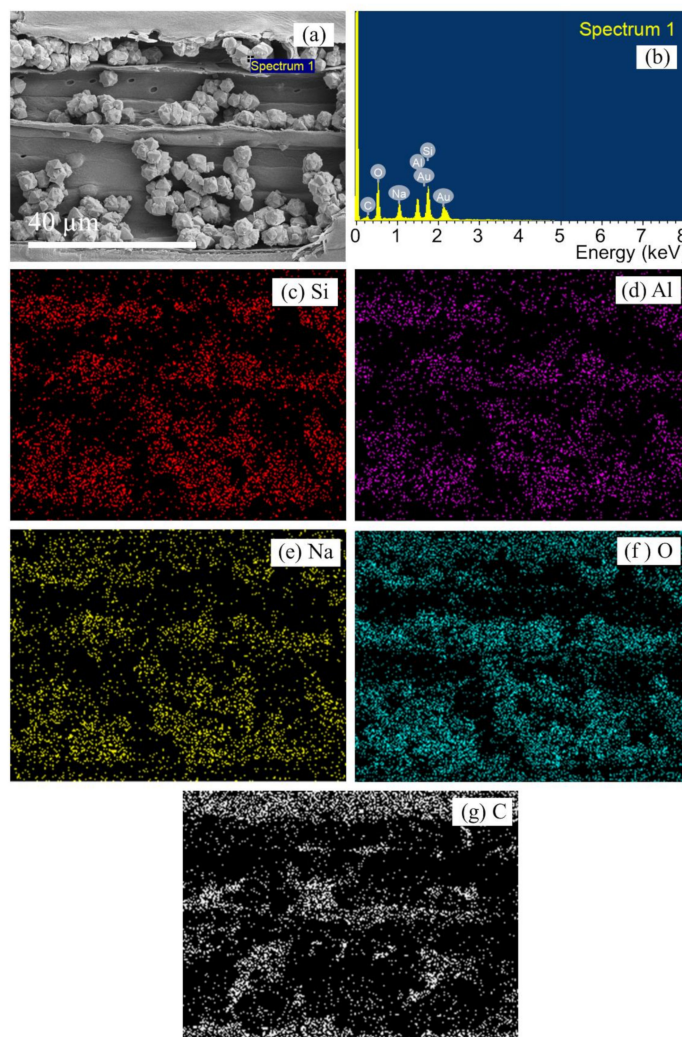


Figure 7. SEM-EDS elemental mapping of refluxed wood-zeolite composite with sonication (RS) (a) SEM image, (b) EDS spectrum, distribution of (c–g).

The Si/Al ratio of this sample is 2.16. The distributions of Si, Al, Na, and O are consistent with each other, indicating the primary atoms of zeolite. The C and O distribution in the upper band corresponds to that of the lignocellulose from Lead tree wood. This confirmed the distribution of zeolite NaY in refluxed LW.

Table 1 summarizes the Si/Al ratio, weight percent, and type of zeolites in each composite. From the untreated wood, zeolite NaP was produced inside the LW. After the wood with the overall gel was sonicated, a mixed phase of zeolite NaP was produced as the main phase, along with NaY. In the case of refluxed wood, NaY was produced. The sonication led to a greater amount of zeolite NaY inside the wood. Thus, the best way to produce NaY inside Lead tree wood is by using acid-refluxed wood and sonication. The percent weight of zeolite ranged between 12.4 and 22.4 g. The trend was not clear because only a small amount of sample, about 15 mg, was used in each measurement. Nevertheless, the results confirmed the success of zeolite synthesis in Lead tree wood.

Table 1. Si/Al ratio from SEM-EDS, weight percent of zeolite per 100 g of composite from TGA and types of zeolites from XRD and SEM.

Samples	Si/Al Ratio	%wt Zeolite in Wood	Zeolite Type	
			From XRD	From SEM
LW	–	0	–	–
Refluxed LW	–	0	–	–
NR	2.25	22.4	NaP	NaP
NRS	2.74 ^a and 2.39 ^b	17.7	NaP + NaY	NaP + NaY
R	2.16	20.4	NaY	NaY
RS	2.16	12.4	NaY	NaY

^a Zeolite NaP; ^b Zeolite NaY.

Figure 8 shows the nitrogen adsorption isotherm of LW, refluxed LW, and as-synthesized composite samples, and Table 2 shows their BET surface areas. The volumes adsorbed on LW and refluxed LW are negligible, suggesting that they are not good adsorbents for nonpolar molecules. The adsorbed volumes on the composites are larger than those of the woods, consistent with the presence of zeolites. The adsorption isotherms are of type I, which is characteristic of zeolites. The BET surface areas are in the following order: NR \approx NRS < R < RS. Because NR and NRS contained NaP, which has a smaller pore size than nitrogen molecules, the adsorbed volumes were small. RS provided the largest adsorbed volumes, implying that it contains NaY more than other samples. Note that the reported surface areas are per mass of the composites, not per mass of the zeolite. So, the values appear lower than typical NaY. Moreover, Table 2 shows the Ni(II) adsorption capacity from all samples. The adsorption capacities are in the following order: NR < NRS < R < RS, consistent with the presence of zeolites and surface areas. In summary, the presence of zeolite in the wood was supported by the data from the adsorption of nitrogen in the gas phase and Ni(II) in the liquid phase. The adsorption increased with the presence of zeolite.

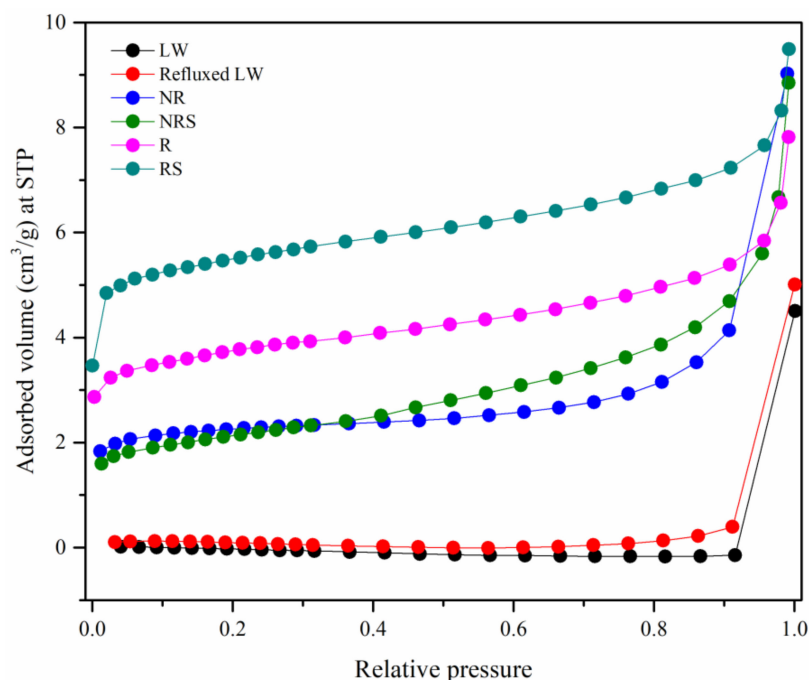
**Figure 8.** Nitrogen adsorption isotherms of Lead tree wood (LW), refluxed LW, Lead tree wood-zeolite composites from untreated wood (NR), untreated wood with sonication (NRS), refluxed wood (R), and refluxed wood with sonication (RS).

Table 2. BET surface area and Ni(II) adsorption capacity.

Samples	S _{BET} (m ² /g)	Ni(II) Adsorption Capacity (mg/g-Adsorbent)
LW	0.2	0.36
Refluxed LW	0.2	0.00
NR	6.4	3.75
NRS	7.0	4.66
R	11.2	5.70
RS	16.1	6.91

4. Conclusions

The composites with zeolite dispersed inside Lead tree wood (LW) are successfully synthesized by two strategies with the gel molar ratio of 10SiO₂:Al₂O₃:4.62Na₂O:180H₂O. Firstly, the untreated wood was used without and with sonication. The products are zeolite NaP and a mixed phase between NaP and NaY. Secondly, refluxed wood was employed without and with sonication. Pure phase zeolite NaY is successfully produced inside LW. The sonication further improves the synthesis, producing more crystals inside the wood. The success of the synthesis was confirmed by X-ray diffraction, scanning electron microscopy, nitrogen adsorption, thermogravimetric analysis, and the adsorption of Ni(II) ions from aqueous solutions.

Author Contributions: Conceptualization, C.K. and J.W.; methodology, P.K. (Panot Krukkratoke), C.K. and P.T.; validation, J.W.; formal analysis, P.K. (Panot Krukkratoke), C.K. and K.P.; investigation, P.K. (Panot Krukkratoke), C.K., P.T., K.P. and J.W.; resources, P.K. (Pongtanawat Khemthong) and J.W.; data curation, P.K. (Panot Krukkratoke), C.K., P.T., P.K. (Pongtanawat Khemthong), S.P. and J.W.; writing—original draft preparation, P.K. (Panot Krukkratoke), C.K., P.T., P.K. (Pongtanawat Khemthong), J.W.; writing—review and editing, P.K. (Panot Krukkratoke), C.K., P.T., P.K. (Pongtanawat Khemthong), S.P. and J.W.; visualization, P.K. (Panot Krukkratoke); supervision, J.W.; funding acquisition, P.K. (Pongtanawat Khemthong) and J.W. All authors have read and agreed to the published version of the manuscript.

Funding: This work is supported by Suranaree University of Technology (SUT). Panot Krukkratoke is supported by Thailand Graduated Institute of Science and Technology (TGIST, Contact No. SCA-CO-2562-9802-TH) and SUT. Pimwipa Tayraukham is supported by the Science Achievement Scholarship of Thailand (SAST). Chalermpan Keawkumay is supported by SUT full-time Doctoral Researcher Grants, Thailand Science Research and Innovation (TSRI), National Science, Research and Innovation Fund (NSRF) (project code 90464).

Institutional Review Board Statement: Not applicable.

Informed Consent Statement: Not applicable.

Data Availability Statement: Not applicable.

Conflicts of Interest: The authors declare no conflict of interest. The funders had no role in the design of the study; in the collection, analyses, or interpretation of the data; in the writing of the manuscript, or in the decision to publish the results.

References

1. Rongchapo, W.; Deekamwong, K.; Loiha, S.; Prayoonpokarach, S.; Wittayakun, J. Paraquat adsorption on NaX and Al-MCM-41. *Water Sci. Technol.* **2015**, *71*, 1347–1353. [[CrossRef](#)] [[PubMed](#)]
2. Rongchapo, W.; Sophiphun, O.; Rintramee, K.; Prayoonpokarach, S.; Wittayakun, J. Paraquat adsorption on porous materials synthesized from rice husk silica. *Water Sci. Technol. J. Int. Assoc. Water Pollut. Res.* **2013**, *68*, 863–869. [[CrossRef](#)]
3. Ismail, A.; Harmuni, H.; Mohd, R.R.M.A.Z. Removal of iron and manganese using granular activated carbon and zeolite in artificial barrier of riverbank filtration. *AIP Conf. Proc.* **2017**, *1835*, 020056.
4. Amin, N.K. Removal of reactive dye from aqueous solutions by adsorption onto activated carbons prepared from sugarcane bagasse pith. *Desalination* **2008**, *223*, 152–161. [[CrossRef](#)]
5. Chaiwon, T.; Jannoey, P.; Channei, D. Preparation of Activated Carbon from Sugarcane Bagasse Waste for the Adsorption Equilibrium and Kinetics of Basic Dye. *Key Eng. Mater.* **2017**, *751*, 671–676. [[CrossRef](#)]
6. Chien, N.D.; Ivanovich, V.A.; Alexandrovna, G.N. Salinity effect on adsorption of phenol by activated carbon from sugarcane bagasse. *Asian J. Chem.* **2019**, *32*, 463–465. [[CrossRef](#)]

7. Oleksiak, M.D.; Ghorbanpour, A.; Conato, M.T.; McGrail, B.P.; Grabow, L.C.; Motkuri, R.K.; Rimer, J.D. Synthesis strategies for ultrastable zeolite GIS polymorphs as sorbents for selective separations. *Chemistry* **2016**, *22*, 16078–16088. [[CrossRef](#)]
8. Fujii, S.; Cha, H.; Kagi, N.; Miyamura, H.; Kim, Y.-S. Effects on air pollutant removal by plant absorption and adsorption. *Build. Environ.* **2005**, *40*, 105–112. [[CrossRef](#)]
9. Erdem, E.; Karapinar, N.; Donat, R. The removal of heavy metal cations by natural zeolites. *J. Colloid Interface Sci.* **2004**, *280*, 309–314. [[CrossRef](#)] [[PubMed](#)]
10. Shariatnia, Z.; Bagherpour, A. Synthesis of zeolite NaY and its nanocomposites with chitosan as adsorbents for lead(II) removal from aqueous solution. *Powder Technol.* **2018**, *338*, 744–763. [[CrossRef](#)]
11. Dotto, G.L.; Meili, L.; Abud, A.K.; Tanabe, E.H.; Bertuol, D.; Foletto, E.L. Comparison between Brazilian agro-wastes and activated carbon as adsorbents to remove Ni(II) from aqueous solutions. *Water Sci. Technol.* **2016**, *73*, 2713–2721. [[CrossRef](#)] [[PubMed](#)]
12. Li, Y.; Li, L.; Yu, J. Applications of zeolites in sustainable chemistry. *Chem* **2017**, *3*, 928–949. [[CrossRef](#)]
13. Li, Y.; Yu, J. Emerging applications of zeolites in catalysis, separation and host–guest assembly. *Nat. Rev. Mater.* **2021**, *6*, 1156–1174. [[CrossRef](#)]
14. Legorreta-Castañeda, A.J.; Lucho-Constantino, C.A.; Beltrán-Hernández, R.I.; Coronel-Olivares, C.; Vázquez-Rodríguez, G.A. Biosorption of Water Pollutants by Fungal Pellets. *Water* **2020**, *12*, 1155. [[CrossRef](#)]
15. Pimsuta, M.; Sosa, N.; Deekamwong, K.; Keawkumay, C.; Thathong, Y.; Rakmae, S.; Junpirom, S.; Prayoonpokarach, S.; Wittayakun, J. Charcoal and wood vinegar from pyrolysis of lead tree wood and activated carbon from physical activation. *Suranaree J. Sci. Technol.* **2018**, *25*, 177–190.
16. Keawkumay, C.; Rongchapo, W.; Sosa, N.; Suthirakun, S.; Koleva, I.Z.; Aleksandrov, H.A.; Vayssilov, G.N.; Wittayakun, J. Paraquat adsorption on NaY zeolite at various Si/Al ratios: A combined experimental and computational study. *Mater. Chem. Phys.* **2019**, *238*, 121824. [[CrossRef](#)]
17. Sosa, N.; Chanlek, N.; Wittayakun, J. Facile ultrasound-assisted grafting of silica gel by aminopropyltriethoxysilane for aldol condensation of furfural and acetone. *Ultrason Sonochem.* **2020**, *62*, 104857. [[CrossRef](#)]
18. Li, J.; Lu, Y.; Yang, D.; Sun, Q.; Liu, Y.; Zhao, H. Lignocellulose aerogel from wood-ionic liquid solution (1-allyl-3-methylimidazolium chloride) under freezing and thawing conditions. *Biomacromolecules* **2011**, *12*, 1860–1867. [[CrossRef](#)]
19. Pimsuta, M. Nickel Phosphide on Activated Carbon for Hydrodeoxygenation of Palm Oil. Ph.D. Thesis, Suranaree University of Technology, Nakhon Ratchasima, Thailand, 2016.
20. Joksimovic, G.; Marković, Z. Investigation of the mechanism of acidic hydrolysis of cellulose. *Acta Agric. Serbia* **2007**, *12*, 51–57.
21. Huo, Z.; Xu, X.; Lü, Z.; Song, J.; He, M.; Li, Z.; Wang, Q.; Yan, L. Synthesis of zeolite NaP with controllable morphologies. *Microporous Mesoporous Mater.* **2012**, *158*, 137–140. [[CrossRef](#)]
22. Khabuanchalad, S.; Khemthong, P.; Prayoonpokarach, S.; Wittayakun, J. Transformation of zeolite NaY synthesized from rice husk silica to NaP during hydrothermal synthesis. *Suranaree J. Sci. Technol.* **2008**, *15*, 225–231.
23. Tayraukham, P.; Jantarit, N.; Osakoo, N.; Wittayakun, J. Synthesis of Pure Phase NaP2 Zeolite from the Gel of NaY by Conventional and Microwave-Assisted Hydrothermal Methods. *Crystals* **2020**, *10*, 951. [[CrossRef](#)]
24. Bunmai, K.; Osakoo, N.; Deekamwong, K.; Kosri, C.; Khemthong, P.; Wittayakun, J. Fast synthesis of zeolite NaP by crystallizing the NaY gel under microwave irradiation. *Mater. Lett.* **2020**, *272*, 127845. [[CrossRef](#)]
25. Shirazian, S.; Parto, S.G.; Ashrafizadeh, S.N. Effect of water content of synthetic hydrogel on dehydration performance of nanoporous LTA zeolite membranes. *Int. J. Appl. Ceram. Technol.* **2014**, *11*, 793–803. [[CrossRef](#)]
26. Wittayakun, J.; Khemthong, P.; Prayoonpokarach, S. Synthesis and characterization of zeolite NaY from rice husk silica. *Korean J. Chem. Eng.* **2008**, *25*, 861–864. [[CrossRef](#)]
27. Bu, N.; Liu, X.; Song, S.; Liu, J.; Yang, Q.; Li, R.; Zheng, F.; Yan, L.; Zhen, Q.; Zhang, J. Synthesis of NaY zeolite from coal gangue and its characterization for lead removal from aqueous solution. *Adv. Powder Technol.* **2020**, *31*, 2699–2710. [[CrossRef](#)]